

Structural Correlations and Mechanical Behavior in Nanophase Silica Glasses

Timothy Campbell, Rajiv K. Kalia, Aiichiro Nakano, Fuyuki Shimojo, Kenji Tsuruta, and Priya Vashishta

*Concurrent Computing Laboratory for Materials Simulations, Department of Physics and Astronomy and
Department of Computer Science, Louisiana State University, Baton Rouge, Louisiana 70803-4001*

Shuji Ogata

Department of Applied Sciences, Yamaguchi University, 2557 Tokiwadai, Ube 755-8611, Japan

(Received 21 September 1998)

Sintering, structural correlations and mechanical behavior of nanophase silica glasses are investigated using large-scale, parallel molecular-dynamics simulations. During the sintering process, the pore sizes and distribution change without any discernible change in the pore morphology. The height and position of the first sharp diffraction peak in the neutron static structure factor shows significant differences in the nanophase glasses relative to the bulk silica glass. The effect of densification on mechanical properties is also examined. [S0031-9007(99)09108-5]

PACS numbers: 61.43.Bn, 61.43.Fs, 61.46.+w

In recent years, cluster-assembled nanophase materials have spurred a great deal of interest in the materials science community. The possibility of tailoring physical properties by controlling the size and distribution of nanoclusters has far-reaching technological implications; in particular, it may be possible to synthesize materials with unique mechanical, electrical, magnetic, and optical properties. Hitherto, a great deal of research has focused on understanding the role of ultrafine microstructures in the physical and chemical behavior of nanophase materials [1]. Much of this research deals with nanocrystalline solids comprising randomly oriented and randomly positioned nanocrystals. It is also of interest to consider non-crystalline nanophase solids formed by the consolidation of nanometer size amorphous clusters. The structure of nanophase amorphous materials is observed to be quite different from that of bulk amorphous solids [2,3].

In this Letter we report on our investigation of nanophase amorphous SiO_2 (*a*- SiO_2 or silica glass) using large-scale molecular-dynamics (MD) simulations on parallel computers. By sintering at different pressures, we have generated nanophase solids with densities ranging from 76% to 93% of the bulk amorphous density (2.2 g/cm^3). In these nanophase *a*- SiO_2 solids, the distribution and structure of micropores, mechanical behavior, and the effects of nanoscale structures on the short-range and intermediate-range order (SRO and IRO) are investigated. Pores in nanophase *a*- SiO_2 are found to have a self-similar structure with a fractal dimension close to 2; pore surface width scales with volume as $W \sim \sqrt{V}$. The MD simulations reveal that the SRO in nanophase silica glass is very similar to that in the bulk glass: both kinds of solids consist of corner-sharing $\text{Si}(\text{O}_{1/2})_4$ tetrahedra. However, the IRO in nanophase silica glass is quite different from that in the bulk. In the nanophase silica glasses the first sharp diffraction peak (FSDP), the signature of IRO [4,5], has a much smaller

height and is shifted to smaller wave vectors relative to the FSDP in the bulk silica glass. From the partial static structure factors and pair-distribution functions, we find that Si-O and Si-Si correlations in the range of 4–10 Å are primarily responsible for the differences in the IRO of bulk and nanophase silica glasses. We have also investigated the mechanical behavior of nanophase *a*- SiO_2 . The elastic moduli are found to have a power-law dependence on the density with an exponent of 3.5. These results are in excellent agreement with experimental measurements on high-density silica aerogels.

The MD simulations reported in this paper are based on an effective interatomic potential that consists of both two-body and three-body interactions. The two-body contribution incorporates atomic sizes via steric repulsion, charge transfer via screened Coulomb potential, and electronic polarizability via charge-dipole interaction. The three-body covalent contribution incorporates bond bending and bond stretching effects. The parameters used in the interaction potential for this work are described in Ref. [6]. This interaction scheme has been validated by comparing the results of MD simulations with a variety of experimental results [7–9].

Nanophase *a*- SiO_2 was synthesized by consolidating an assembly of *a*- SiO_2 clusters under constant temperature and pressure. The initial *a*- SiO_2 cluster was obtained by removing a spherical cluster 7 nm in diameter (10 905 atoms) from well-thermalized bulk *a*- SiO_2 . Subsequently, the steepest-descent quench was applied to bring the atoms in the cluster to the zero-force configuration. The cluster was then gradually heated to 1000 K. The initial nanophase MD configuration was generated by randomly positioning (with random orientations) 100 of these spherical *a*- SiO_2 clusters at 1000 K in a cubic box 36 nm on the side [10]. The initial mass density was 0.79 g/cm^3 . Simulations were performed in the isothermal-isobaric ensemble. The equations of motion were integrated with a

reversible multiple time-scale algorithm using a time step of 2 fs [11]. First, at zero pressure and 1000 K, the entire system was relaxed for 22 000 time steps. The pressure was then increased to 0.1 GPa and the system was further thermalized for 30 000 steps. Subsequently, the pressure was increased to 0.8, 1.6, and 2.4 GPa and at each pressure the system was thermalized for 10 000 steps. The three systems at 0.8, 1.6, and 2.4 GPa were cooled slowly to 200 K and then the external pressures were removed gradually. In each case the volume increase upon removing the pressure was no more than 7%. In this manner, we obtained nanophase a -SiO₂ with mass densities of 1.73, 1.90, and 2.03 g/cm³ at 200 K. A fourth system with mass density of 1.65 g/cm³ was obtained in a similar manner by thermalizing at a pressure of 0.6 GPa.

Figure 1 shows a 3D color plot of pores in two of the four nanophase silica glasses (the pores are shown in cyan). (The pores are identified by subdividing the MD box into 4 Å voxels and then performing a clustering analysis on the empty voxels using a breadth-first-search algorithm; this analysis was done at 5 K.) The nanophase system at the lower density (1.67 g/cm³) contains many pores including a percolating pore, which occupies 36% of the total pore volume. Note that a pressure of 2.4 GPa the system achieves 93% of the bulk silica glass density. This well-consolidated system contains only small isolated pores.

Despite the differences in the pore sizes and distribution, we find remarkable similarity in the morphology of pores in nanophase a -SiO₂ at different densities. The pore morphology is defined in terms of the fractal dimension of pores and the roughness exponents of pore/silica interfaces. The average pore radius is calculated from

$$R^2 = \frac{1}{N_S} \sum_{i=1}^{N_S} |\vec{r}'_i - \vec{r}_0|^2, \quad \vec{r}_0 = \frac{1}{N_V} \sum_{i=1}^{N_V} \vec{r}_i, \quad (1)$$

where \vec{r}_0 is the center of the pore, and $\{\vec{r}_i\}$ and $\{\vec{r}'_i\}$ denote the centers of voxels inside and at the interface of the pore, respectively. The roughness of pore interfaces is

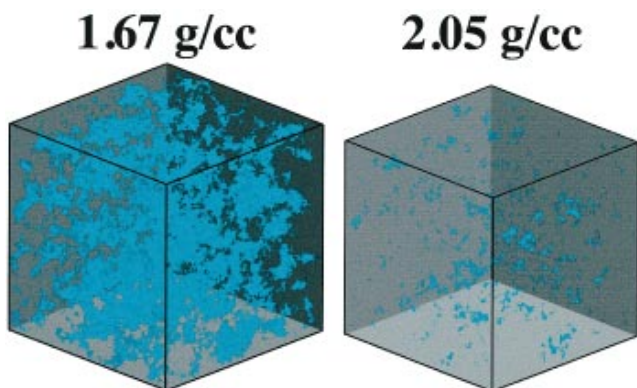


FIG. 1(color). Pores in nanophase a -SiO₂ at mass densities 1.67 and 2.05 g/cm³. The pores are shown in cyan.

obtained from the interface width W [12],

$$W = \left\{ \frac{1}{N_S} \sum_{i=1}^{N_S} (|\vec{r}'_i - \vec{r}_0| - R)^2 \right\}^{1/2}. \quad (2)$$

Figure 2 shows a log-log plot of R and W as a function of the pore volume V for the nanophase system at 1.92 g/cm³. The MD results for the average radius and the interface width obey the power-law behavior: $R \sim V^\eta$ and $W \sim V^\mu$, with the best fit being $\eta = 0.47 \pm 0.02$ and $\mu = 0.51 \pm 0.02$. The fractal dimension of the pores is $d = 1/\eta = 2.1 \pm 0.09$. Within the statistical uncertainty, we find no difference in the fractal dimension or the roughness exponent of pores in nanophase a -SiO₂ at different densities.

The MD calculations reveal insignificant differences in the SRO of nanophase silica glasses when compared with the bulk glass. All of the nanophase systems have corner-sharing Si(O_{1/2})₄ tetrahedral units similar to the bulk silica glass. In the nanophase systems the nearest-neighbor distances, coordinations, and bond angle distributions in the cluster interiors and interfacial regions are very similar. The nearest neighbor Si-Si, Si-O, and O-O distances are found to be 3.10, 1.65, and 2.64 Å, respectively. The O-Si-O and Si-O-Si bond angle distributions have peaks around 109° and 144°, respectively (the distributions for the interfacial regions are slightly broader in comparison to the interior regions).

The most dramatic change in structural correlations is observed in the FSDP in the neutron-scattering static structure factor, $S_n(k)$. The FSDP yields information about the IRO in glasses [4,5]. In the past decade it has been the focus of many experimental and computer simulation studies of amorphous silica as well as other oxide and chalcogenide glasses. Figure 3 shows a comparison of $S_n(k)$ calculated from MD simulations (solid line) and neutron-scattering measurements (solid dots) [13] for bulk a -SiO₂. Our MD simulations for bulk a -SiO₂ have been

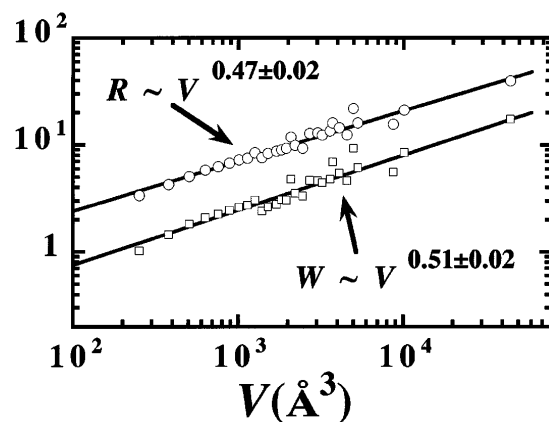


FIG. 2. Log-log plot of the average pore radius (R) and interface width (W) as a function of the pore volume (V). Solid lines are best least-squares fits.

shown previously to be of the highest quality by quantitatively comparing the simulation results with experiments in terms of the R_χ quality factor introduced by Wright [14]. The R_χ factor for the comparison of our MD simulations with experiment is 4.4% [9], which is the lowest of all the available MD simulations of silica glasses.

Figure 3 also shows the MD results for $S_n(k)$ for nanophase silica glasses at various densities. Variations in $S_n(k)$ as a function of density are prominent in the wave-number region $k < 2 \text{ \AA}^{-1}$, whereas no significant differences are found for $k > 2 \text{ \AA}^{-1}$. As seen in the Fig. 3 (inset) the height of the FSDP in the nanophase glasses is significantly smaller than that of the bulk silica glass. Additionally, the position of the FSDP in nanophase silica glasses shifts toward smaller k with respect to the bulk.

We have analyzed the differences in the IRO of nanophase and bulk silica glasses by examining the partial static structure factors. Figure 4 shows how the height and the position of the FSDP and the partial contributions to the FSDP vary as a function of the density. We note that in the nanophase silica glasses the height of the FSDP in $S_n(k)$ increases gradually with density. This behavior reflects the trend seen in the Si-O contribution to the height of the FSDP. The Si-Si and O-O contributions to the height of the FSDP are flat with respect to density. The most remarkable feature is that the height of the FSDP for bulk silica glass is at least 15% higher than that of the nanophase glasses. The position of the FSDP in the

nanophase glasses is observed to move toward larger k as the density increases. This behavior is reflected in the Si-O and O-O contributions, whereas the Si-Si contribution to the FSDP position is unchanged with density. For fully consolidated nanophase silica glasses (at the same density as the bulk glass), the position of the FSDP is expected to be very close to the FSDP position in the bulk silica glass.

The behavior of the position of the FSDP can be understood through detailed analyses of the partial pair-distribution function $g_{\alpha\beta}(r)$. Figure 5 shows a plot of $\langle n_{\alpha\beta}(r) \rangle = 4\pi\rho_\beta r^2 g_{\alpha\beta}(r)$, where ρ_β is the partial number density of the species β . The solid straight lines are drawn to show the general trend of the peaks in the 4–10 Å range as the density changes. In the case of Si-Si, the decrease in the density causes the second-peak position around 5 Å to shift toward larger distances and the third- and the fourth-peak positions to shift toward smaller distances. These shifts in opposite directions nullify and hence the position of the Si-Si FSDP is insensitive to variations in the density of nanophase silica glasses [Fig. 4 (bottom)]. The second, third, and fourth peaks for the Si-O and O-O pair-distribution functions shift toward larger r as the density decreases. This is consistent with the density dependencies of the FSDP positions for Si-O and O-O pairs shown in Fig. 4 (bottom).

We have also investigated the effect of densification on the elastic moduli of nanophase silica glass. Figure 6 shows a log-log plot of the bulk (K), shear (G), and Young's (E) moduli for the nanophase and bulk silica

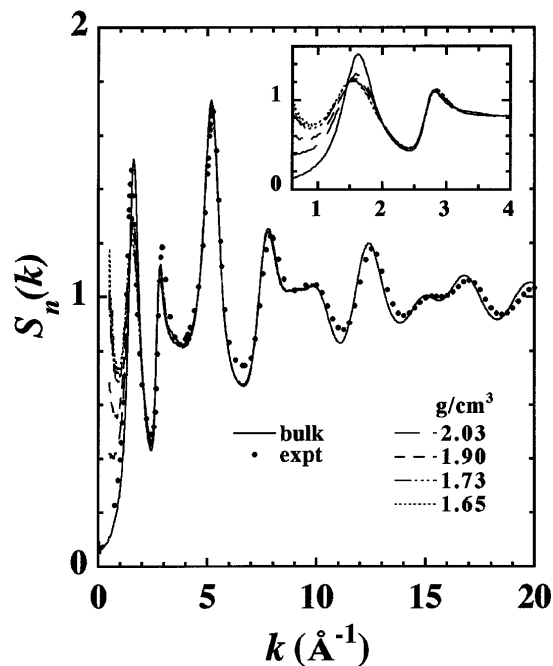


FIG. 3. Neutron-scattering static structure factor, $S_n(k)$, for bulk and nanophase $a\text{-SiO}_2$. Solid and dashed lines, MD results; solid dots, neutron-diffraction experiments for bulk $a\text{-SiO}_2$ (Ref. [13]). Inset: magnification of the FSDP region.

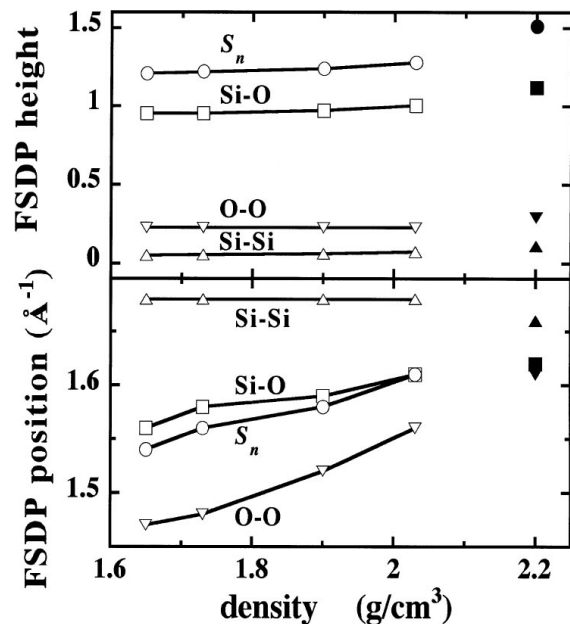


FIG. 4. MD results for height and position of the FSDP and the partial contributions (Si-Si, Si-O, and O-O) to the FSDP in $S_n(k)$ for bulk and nanophase $a\text{-SiO}_2$. Open symbols, nanophase $a\text{-SiO}_2$; solid symbols, bulk $a\text{-SiO}_2$.

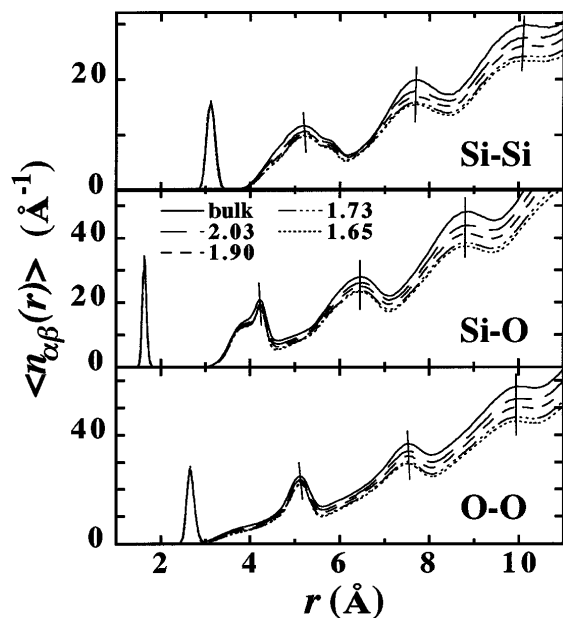


FIG. 5. Plot of $\langle n_{\alpha\beta}(r) \rangle = 4\pi\rho_{\beta}r^2g_{\alpha\beta}(r)$ for bulk and nanophase α -SiO₂. The solid straight lines show the general trend of the peaks as the density varies.

systems as a function of the density, $\bar{\rho}$, relative to the bulk silica density. The solid lines are the best least-squares fits for each of the moduli. We find that the elastic moduli scale as $\bar{\rho}^{3.5 \pm 0.2}$. These simulation results are in excellent agreement with experimental measurements in silica aerogels, which show the power-law dependence of elastic moduli on the density with the exponent for the high-density aerogels and nonporous silica being 3.49 [15].

In conclusion, using parallel computers we have carried out large-scale MD simulations to investigate how solids synthesized by the consolidation of glassy silica nanoclusters are different from the bulk SiO₂ glass. In nanophase silica glasses with densities ranging from 76% to 93% of the bulk amorphous density, we find the structure of pores to be self-similar with a fractal dimension close to 2 and surface roughness exponents of pores to be always ~ 0.5 . The SRO in nanophase glasses is similar to the bulk glass. However, the IRO is quite different in these two classes of solids. The FSDP in nanophase glasses is observed to have a much smaller height and is shifted toward smaller k relative to the FSDP in the bulk silica glass. The elastic moduli of nanophase silica glasses scale with the density as $M \sim \rho^{3.5}$. The predictions of the MD simulations with regard to the IRO and mechanical behavior can be verified by neutron-scattering experiments and the measurement of elastic moduli of nanophase silica glasses.

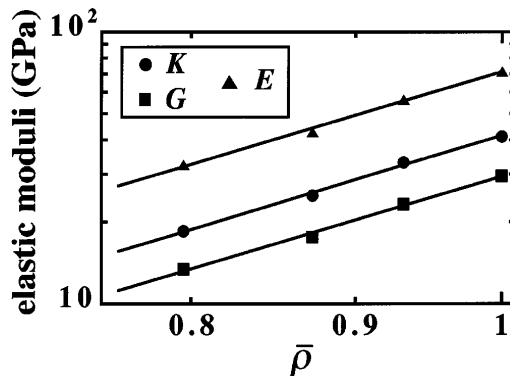


FIG. 6. Log-log plot of the bulk (K), shear (G), and Young's (E) moduli for bulk and nanophase α -SiO₂ as a function of the density relative to the bulk density. The solid lines are best least-squares fits for each of the moduli.

This work was supported by NSF, U.S. DOE, Air Force Office of Scientific Research, Army Research Office, USC-LSU Multidisciplinary University Research Initiative, Petroleum Research Fund, NSF-JSPS USA-Japan International Grant, and Louisiana Education Quality Support Fund. Simulations were performed on the 56-processor DEC Alpha cluster in the Concurrent Computing Laboratory for Materials Simulations at Louisiana State University, and on the 128 node SGI Origin 2000 at ASC MSRC.

- [1] R. W. Siegal, *J. Phys. Chem. Solids* **55**, 1097 (1994).
- [2] J. Jing *et al.*, *J. Non-Cryst. Solids* **113**, 167 (1989).
- [3] J. Weissmuller *et al.*, *Phys. Lett. A* **145**, 130 (1990).
- [4] S. C. Moss and D. L. Price, in *Physics of Disordered Materials*, edited by D. Adler, H. Fritzsche, and S. R. Ovshinsky (Plenum, New York, 1985), p. 77.
- [5] S. R. Elliott, *Phys. Rev. Lett.* **67**, 711 (1991).
- [6] P. Vashishta *et al.*, in *Amorphous Insulators and Semiconductors*, edited by M. F. Thorpe and M. I. Mitkova (Kluwer Academic, Dordrecht, The Netherlands, 1997), p. 151.
- [7] P. Vashishta *et al.*, *Phys. Rev. B* **41**, 12 197 (1990).
- [8] W. Jin *et al.*, *Phys. Rev. B* **48**, 9359 (1993).
- [9] A. Nakano *et al.*, *J. Non-Cryst. Solids* **171**, 157 (1994).
- [10] The initial "random" cluster positions were generated from a Monte Carlo simulation consisting of 100 particles with sufficient size to prevent overlap of the clusters in the MD box.
- [11] G. J. Martyna *et al.*, *Mol. Phys.* **87**, 1117 (1996).
- [12] M. Plischke and Z. Rácz, *Phys. Rev. Lett.* **53**, 415 (1984).
- [13] P. A. V. Johnson *et al.*, *J. Non-Cryst. Solids* **58**, 109 (1983).
- [14] A. C. Wright, *J. Non-Cryst. Solids* **159**, 264 (1993).
- [15] J. Groß and J. Fricke, *Nanostruct. Mater.* **6**, 905 (1995).